Earth Planets Space, **61**, 71–81, 2009

Gilbert-Gauss geomagnetic reversal recorded in Pliocene volcanic sequences from Georgia (Lesser Caucasus): revisited

Avto Goguitchaichvili[1]*, Miguel Angel Cervantes[1], Manuel Calvo Rathert[2], Pierre Camps[3], Jemal Sologashvili[4], and Givi Maissuradze[5]

[1]*Laboratorio Interinstitucional de Magnetismo Natural, Instituto Geofísica—Sede Michoacán, Universidad Nacional Autónoma de México, Morelia, Mexico*
[2]*Departamento de Física, Universidad de Burgos, Av. Cantabria, s/n, 09006 Burgos, Spain*
[3]*Geoscience Montpellier, Université Montpellier 2, Case 049, 34095 Montpellier, Cedex 5, France*
[4]*Tbilisi State University Ivane Djavakhishvili, 3, Tshavtshavadze St., 380064 Tbilisi, Georgia*
[5]*Institute of Geology, Alexidze 9, 380009 Tbilisi, Georgia*

(Received October 23, 2007; Revised July 23, 2008; Accepted August 2, 2008; Online published January 23, 2009)

We carried out a detailed paleomagnetic, rock-magnetic, and Thellier paleointensity study of an ∼3.6 My Pliocene lava flow succession in southern Georgia. An earlier study (Camps *et al.*, 1996) revealed that several consecutive lava flows record an intermediate polarity direction at the base of the section followed by a thick reverse polarity zone. The transitional field was interpreted as an excursion within chron 2Ar or an upper Cochiti-Gilbert reversal. New paleomagnetic data reported here have been obtained from nearby lava successions. In total, about 170 standard paleomagnetic cores belonging to 22 lava flows were collected during the 2005 sample collection campaign. Rock-magnetic experiments showed that the remanence is carried by Ti-poor titanomagnetite in most of the samples. The fraction of grains with multidomain magnetic structure does not seem to be important. Characteristic remanent magnetization was successfully determined on all samples. The direct correlation with the original (Thoki) sequence, previous preliminary measurements of natural remanent magnetization (Sologashvili, 1986), and field observations allowed us to establish a new magnetic stratigraphy. The lower part of section is characterized by intermediate magnetic polarity followed by thick reversely magnetized lavas. The upper sequence, represented by 18 consecutive flows yielded normal magnetic polarity. The mean paleointensity of the intermediate field is drastically reduced with respect to the post-transitional field strength. Based on all available radiometric ages and new paleomagnetic data, it may be speculated that Gilbert-Gauss (R-N) reversal was recorded at the upper part of sequence. Lower intermediate polarity flows possibly represent a form of precursor of this reversal that is similar to the Matuyama-Brunhes geomagnetic transition.

Key words: Paleomagnetism, reversals, excursions, paleointensity, Caucasus.

1. Introduction

The Earth's magnetic field has often shown wide departures from its usual axial dipole configuration for relatively brief periods of about 3×10^3 years (Gubbins, 1999). This fundamental property of the Earth's magnetic field is known as a geomagnetic excursion. Slightly larger intervals (5×10^3 to 7×10^3 years) during which the geomagnetic field switches its polarity following widely different paths for different transitions are of particular importance in furthering in our understanding of the physical process in the Earth's deep interiors. Cox (1968) predicted that there should be numerous undiscovered geomagnetic reversals and excursions in the Brunhes chron. The most recent geomagnetic instability time scale (GITS) proposed to describe the geochronology of such excursions (Singer *et al.*, 2002; Petronille *et al.*, 2005) contains evidence for 14 geomagnetic excursions in the Brunhes. However, only five events (Laschamps, Blake, Jamaica, Calabrian Ridge, and Big Lost) are documented by paleomagnetic and high-resolution geochronology studies using volcanic rocks. A polarity transition takes place very rapidly with respect to the geological timescale. Thus, it is difficult to find rocks that have preserved a complete and accurate record. Absolute paleointensity determinations may be obtained exclusively from volcanic rocks, but in many cases there is little stratigraphic control. Sediments, in contrast, may provide good chronological control but they may be occasionally altered by various chemical perturbations (Tauxe, 1993; Dunlop and Özdemir, 1997; Goguitchaichvili *et al.*, 1999a). Ideally, the presence of geomagnetic events should be confirmed or completed by information from lava flows (Merrill and McFadden, 1994; Valet and Herrero-Bervera, 2003; Knudsen *et al.*, 2003).

While many geomagnetic events are revealed and radiometrically dated within the Bruhnes chron (e.g., Mochizuki *et al.*, 2006, 2007; Gratton and Shaw, 2007), other periods remain relatively poorly studied. This is particularly true

*Current address (sabbatical): Departamento de Geologia y Mineralogia, Instituto de Investigaciones Metalurgicas, Universidad Michoacana de San Nicolas de Hidalgo, Mexico.

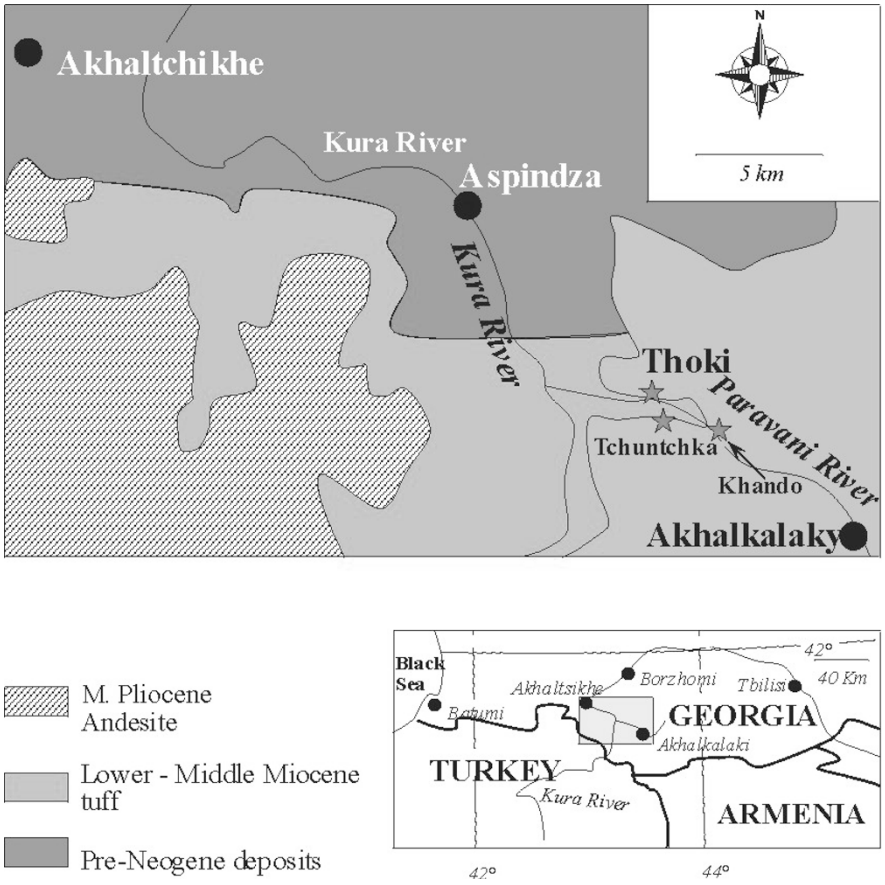

Fig. 1. Simplified geologic map of Akhalkalaki region showing location of main sampling sites (adopted from Camps *et al*. (1996) and Goguitchaichvili *et al*. (2001b)).

for the Gilbert chron, which still may be considered to be poorly studied. We present here a detailed paleomagnetic, rock-magnetic, and Thellier paleointensity study of an Ar-Ar dated lava flow succession located in southern Georgia. A previous study (Camps *et al*., 1996) revealed that several consecutive lava flows record an intermediate polarity direction at the base of the section followed by a thick reverse polarity zone. Here, we try to extend the paleomagnetic record by sampling some parallel sequences that may be unambiguously correlated to the original profile. In addition, we succeeded in estimating the absolute paleointensity—a decisive parameter in furthering our understanding of the field behavior during and around reversals and excursions.

2. Geological Context and Sampling

Alpine, late Miocene to Holocene compression is responsible for intensive volcanic activities in the southern Caucasus (Maissuradze, 1989). According to geological and petrological studies (Milanovski, 1978), three phases of volcanic activity can be distinguished: (1) late Miocene to early Pliocene, (2) middle to late Pliocene or Pleistocene, and (3) Quaternary. In the southern Caucasus, post-orogenic subaerial volcanism occurred in four main areas: the south Georgian volcanic province, the Khrami basin, the small Caucasus, and the Kazbeki region. The Akhalkalaki volcanic area, which is the subject of the present study, is located in the western part of the south Georgian volcanic province (Fig. 1) and lies discordantly on the Goderzi Miocene volcanic tuffs. Its lower units (defined as the Lower Akhalkalaki Sequence by Milanovski, 1978) are made up of doleritic basaltic and, less frequently, of basaltic-andesitic lava flows (Sologashvili, 1986; Camps *et al*., 1996). Most of the ages are assigned to the Pliocene, but magmatic activity did continue during the Quaternary. The Ar-Ar dating of plagioclases from three flows located in the lower part of the Akhalkalaki Plateau yielded an average age of about 3.6±0.06 Ma (Camps *et al*., 1996).

The original Thoki section studied by Camps *et al*. (1996) is situated at 41°28.616N latitude and 43°22.850E, about 1 km S-SE of the village of Thoki and the Tchobareti brook confluent (Fig. 1). This formation consists of two parts, the Lower and Upper Akhalkalaki Sequences, which are clearly separated by an erosion surface. Due to the time needed for erosion, there is no doubt that some relatively large period of quiescence occurred between the lava emissions of the Lower and Upper Akhalkalaki Sequences. This study focused only on the Lower Akhalkalaki Sequence. At the Thoki site, the Lower Akhalkalaki Sequence is approximately 250 m thick and composed of 24 gray, massive, and coarse-grained lava flows with a maximum thickness of about 30 m. Camps *et al*. (1996) reported that lower lava flows provide intermediate polarity directions, while the upper part is reversely magnetized. The Tchuntchka section (41°28.566N, 43°23.078E) is located at a distance of about 1 km (Fig. 1) from the Thoki main section. Its approximate thickness is estimated as 300 m, and it comprises at least 32

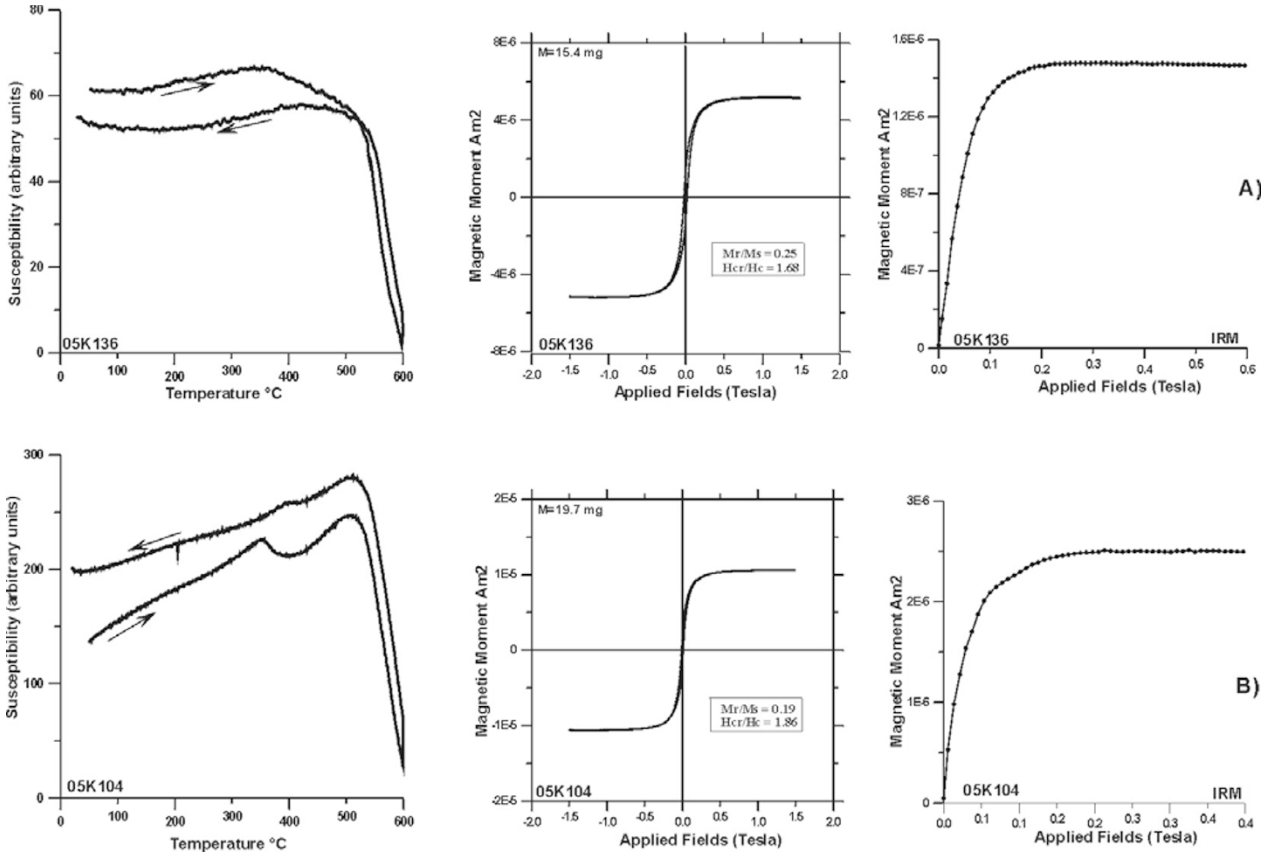

Fig. 2. Examples of rock-magnetic experiments: susceptibility versus temperature (in air) curves of representative samples (the arrows indicate the heating and cooling curves) and typical examples of hysteresis loops (uncorrected for dia and paramagnetic contributions) with associated isothermal remanence (IRM) acquisition curves of small chip samples from the studied volcanic units.

lava flows. We note that the much younger Upper Akhalkalaki Sequence is not present here. No evidence of erosion surface, paleosol development, or sedimentation has been observed between these consecutive lava flows. Goguitchaichvili *et al*. (1997) reported reverse polarity directions at the middle part of sequences followed by thick normal polarity lavas. Due to accessibility difficulties, the lower part of sequence remained unstudied. The Khando section (41°28.218N, 43°24.126E), in contrast, is represented by both the Lower and Upper Akhalkalaki Sequences. Here, the total thickness is only 170 m and comprises 16 consecutive lava flows.

During the 2005 campaign we succeeded in collecting about 50 standard paleomagnetic cores (six lava flows) from the lower part of Tchuntchka section while 16 consecutive flows (128 samples) were sampled at Khando site. The upper part of Khando, similarly to Thoki, is clearly younger, and the erosion surface is well-defined. The samples are distributed throughout each flow both horizontally and vertically in order to minimize the effects of block tilting and lightning. Many cores were drilled at the very bottom of the flows with the hope of collecting samples with the finest grained material. Standard paleomagnetic cores were obtained with a gasoline-powered portable drill and oriented with both magnetic and sun compasses.

3. Rock Magnetic Properties

In order to identify the magnetic carriers responsible for the remanent magnetization and to obtain information about their paleomagnetic stability, we performed several rock-magnetic experiments. These experiments included: (1) measurements of the viscosity index, (2) measurements of thermomagnetic curves (susceptibility versus temperature), and (3) hysteresis experiments.

3.1 Viscosity index

Determination of the viscosity index (Thellier and Thellier, 1944; Prévot *et al*., 1983) allows estimation of the capacity of a sample to acquire a viscous remanent magnetization and is therefore a useful tool for obtaining information on the paleomagnetic stability of the sample. To this end, we positioned samples so that one of their axes was aligned with Earth's magnetic field and left them for 16 days. After we had measured their magnetization (M_d), we placed place for a second 16-day period in a field-free space and again measured their magnetization (M_0). These two values were then used to calculate the viscosity index $V = [(Z_\mathrm{d} - Z_0) : M_\mathrm{nrm}] \times 100$, where Z_d and Z_0 are the magnetization components of M_d and M_0, respectively, which are parallel to the magnetizing field, and M_nrm is the intensity of the natural remanent magnetization. These experiments were performed on three samples from each unit, and although the viscosity indexes varied between 0 and 14.8, most values were found to be lower than 5% (average value: 3.2%). Generally speaking, the studied samples

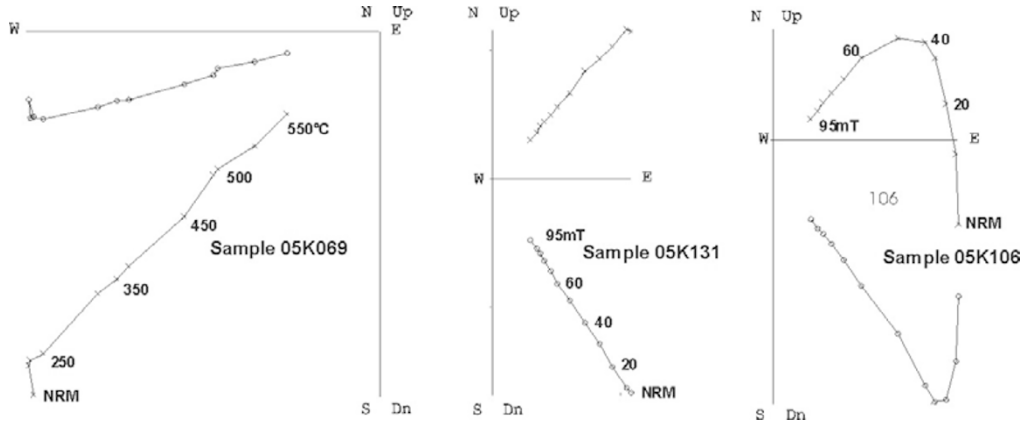

Fig. 3. Orthogonal vector plots of stepwise thermal or alternating field demagnetization of representative samples (stratigraphic coordinates). The numbers refer either to the temperatures (in °C) or to peak alternating fields (in mT). o, Projections into the horizontal plane; x, projections into the vertical plane.

Table 1. Flow mean directions of cleaned remanence for the Tchunchka and Khando profiles. N, number of treated samples; n, number of specimens used for calculation; Dec, Declination; Inc, Inclination. k and α_{95}: precision parameter and radius of 95% confidence cone of Fisher statistics, δ is the angular deviation from the expected mean Pliocene paleodirections; DG, directional groups (see text for more details).

Site	n/N	Inc	Dec	k	α_{95}	δ	DG
Tchuntchka profile							
TH06	7/7	53.4	260.7	326	3.3	53.5	NR3
TH05	5/5	51.7	261.8	177	5.7	54.6	NR3
TH04	6/7	32.1	253.2	210	3.9	74.1	NR1
TH03	7/7	30.1	249.7	503	2.6	77.4	NR1
TH02	8/8	29.9	253.7	239	3.4	77.3	NR1
TH01	7/7	25.9	250.7	174	5.1	80.5	NR1
Khando profile							
XA16	8/8	−30.8	151.4	565	2.8	35.8	NR4
XA15	6/7	−31.6	154.2	296	3.8	33.9	NR4
XA14	6/8	−32.7	149.6	228	5.3	35.1	NR4
XA13	6/6	−29.1	153.4	660	2.3	36.5	NR4
XA12	6/6	−33.2	154.6	212	4.4	32.4	NR4
XA11	6/7	−31.8	159.7	262	4.2	31.5	NR4
XA10	6/6	−27.8	153.3	405	3.9	37.6	NR4
XA09	6/7	−28.2	150.4	465	3.3	38.8	NR4
XA08	6/7	53.2	261.6	163	5.6	53.3	NR3
XA07	6/7	51.4	259.2	251	4.8	55.6	NR3
XA06	8/8	47.7	249.1	342	3.6	62.4	NR2
XA05	5/6	51.2	250.8	96	5.8	58.9	NR2
XA04	6/6	48.8	249.2	612	2.7	61.5	NR2
XA03	7/7	49.2	251.7	212	4.1	60.2	NR2
XA02	7/8	51.4	250.8	166	3.8	58.8	NR2
XA01	7/8	49.9	248.5	319	3.4	60.7	NR2

showed a relatively low capacity for acquiring viscous remanent magnetization.

3.2 Continuous susceptibility curves

Low-field susceptibility measurements (k-T curves) under air were carried out using a Highmoore susceptibility bridge equipped with a furnace. A few samples were treated using the Bartington (MS2) susceptibility versus temperature system. One sample from each site was heated up to about 600°C at a heating rate of 15°C/min and then cooled down at the same rate. The Curie temperature was determined using the method proposed by Prévot *et al.* (1983).

Two different types of behavior were observed during these experiments (Fig. 2): the curves indicate, in most cases, the presence of Ti-poor titanomagnetites (Fig. 2(a), sample 05K136). However, the cooling and heating curves are not perfectly reversible, probably because of a low initial value of magnetic susceptibility and alterations due to the heating in air. A few sites (sample 05K104) apparently show evidence of two ferrimagnetic phases during heating. The lower Curie point ranges between 350 and 400°C and the higher one is about 580°C. The cooling curve shows only a single major phase, with a Curie temperature close to that of magnetite. Such irreversible k-T curves can be explained by the presence of titanomaghemite, which probably transformed into magnetite (Özdemir, 1987) during the heating. In some cases, the low susceptibility signal prohib-

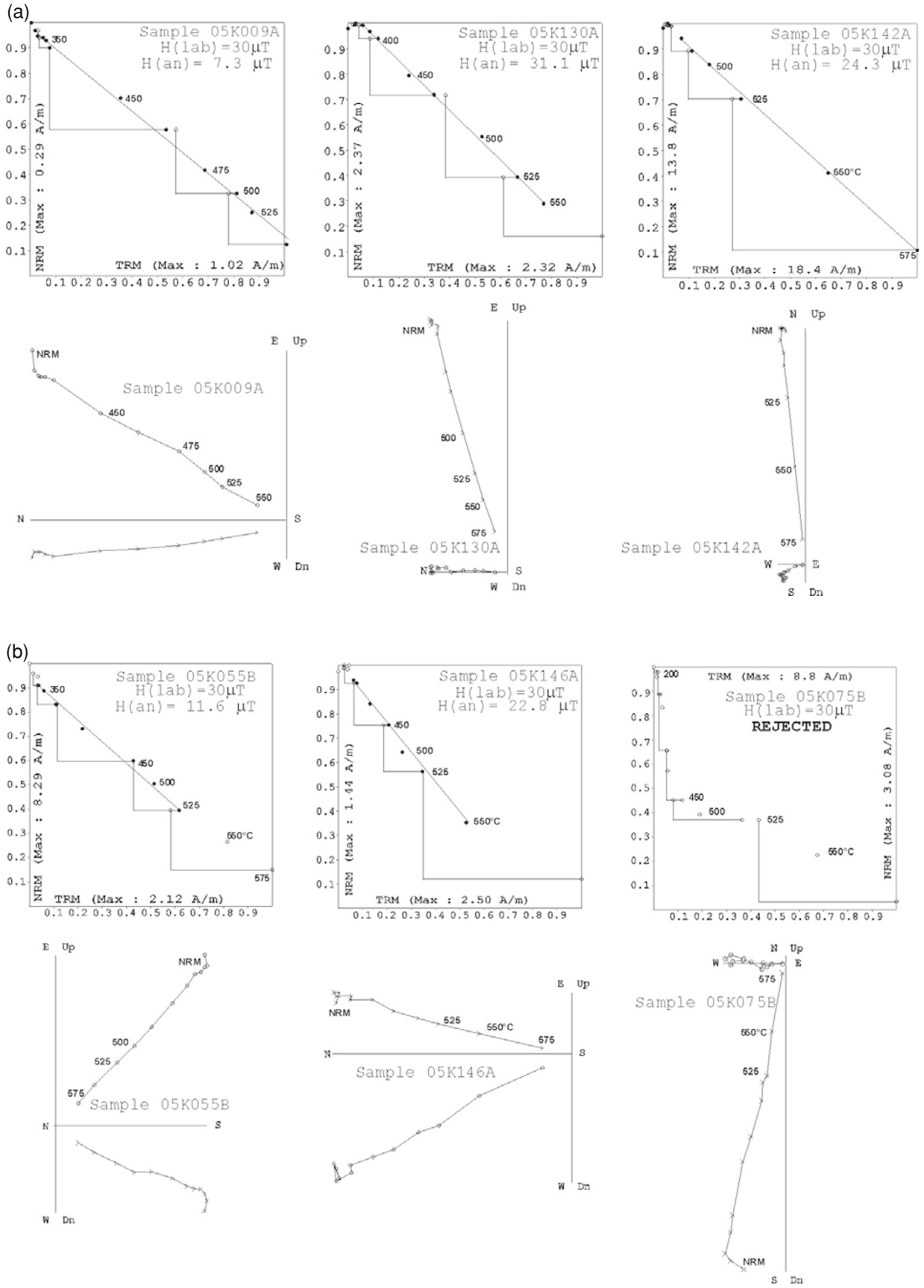

Fig. 4. The representative NRM-TRM plots and associated orthogonal diagrams from Akhalkalaki samples. In the orthogonal diagrams we used same notations as those in Fig. 3. Also shown is an example of the rejected sample.

Table 2. Paleointensity results from Lower Akhalkalaki Sequence (Tchuntchka and Khando profiles) volcanic lava flows. n, number of NRM-TRM points used for palaeointensity determination; T_{min}–T_{max} temperature interval used; f, g, and q are the fraction of extrapolated NRM used, the gap factor and quality factor, respectively; F_E, paleointensity estimate for individual specimen, $\sigma(F_E)$ is the standard error of F_E; F_E, average paleointensity of individual lava flow, with the plus and minus sign corresponding to standard deviation; VDM and VDMe, individual and average virtual dipole moments, respectively.

Site	Sample	n	T_{min}–T_{max}	f	g	q	$F_E \pm \sigma(F_E)$	VDM	$F_E \pm$ s.d.	VDMe
TH01	05K001B	7	250–500	0.64	0.79	10.2	12.5±0.6	3.99	10.2±2.3	2.4±0.6
	05K002B	8	250–525	0.75	0.76	8.9	8.7±0.4	2.68		
	05K006A	7	250–500	0.57	0.77	8.6	12.6±0.6	3.02		
	05K008A	7	350–550	0.76	0.73	9.1	9.8±0.5	2.35		
	05K009A	10	250–575	0.86	0.77	26.6	7.3±0.2	1.75		
TH02	05K011A	9	250–550	0.73	0.84	27.1	8.4±0.2	1.96	9.8±2.3	2.3±0.5
	05K013A	9	300–550	0.51	0.87	14.7	13.1±0.5	3.06		
	05K015A	11	20–575	0.79	0.85	39.2	6.8±0.1	1.59		
	05K016A	6	250–475	0.79	0.68	4.7	10.6±0.5	2.47		
	05K017A	7	300–525	0.63	0.79	23.9	10.1±0.2	2.36		
TH04	05K026A	7	250–500	0.59	0.79	12.6	6.4±0.2	1.47	7.0±0.5	1.6±0.1
	05K030A	8	250–525	0.64	0.83	9.3	7.2±0.4	1.65		
	05K028D	8	300–550	0.72	0.84	15.6	7.4±0.2	1.7		
TH06	05K039A	7	250–500	0.53	0.81	9.2	11.1±0.5	2.06	12.3±1.7	2.3±0.3
	05K040A	8	300–525	0.84	0.77	4.4	13.5±1.8	2.51		
XA02	05K055B	7	300–525	0.82	0.84	12.9	10.3±0.5	1.96	11.6±1.4	2.2±0.2
	05K056B	7	250–500	0.55	0.81	5.8	10.5±0.9	2.0		
	05K057B	8	250–525	0.57	0.78	6.5	12.7±0.8	2.33		
	05K059B	9	200–550	0.49	0.86	10.8	12.9±0.4	2.37		
XA03	05K063A	10	20–550	0.53	0.81	16.3	13.3±0.3	2.6	13.6±1.3	2.7±0.3
	05K064A	8	200–550	0.48	0.86	6.3	15.3±1.1	2.99		
	05K066A	7	250–500	0.46	0.79	6.2	12.1±0.7	2.36		
	05K067A	8	200–550	0.65	0.75	9.4	13.7±0.7	2.68		
XA07	05K091A	10	200–550	0.51	0.85	7.2	13.8±0.8	2.63	12.8±1.1	2.4±0.2
	05K093A	9	250–550	0.51	0.86	10.9	13.1±0.5	2.49		
	05K094A	8	200–525	0.46	0.83	5.7	11.6±0.6	2.21		
XA12	05K129A	7	250–500	0.55	0.77	11.2	34.3±1.3	7.81	32.4±1.7	7.4±0.4
	05K130A	8	300–550	0.67	0.78	26.7	31.1±0.6	7.08		
	05K131C	7	400–550	0.71	0.77	11.6	31.8±1.2	7.24		
XA14	05K143A	6	400–575	0.82	0.81	59.6	22.7±0.2	5.19	22.8±1.4	5.2±0.3
	05K144A	8	300–575	0.88	0.79	33.1	21.5±0.4	4.91		
	05K142A	7	400–550	0.71	0.77	11.6	24.3±1.1	5.55		
XA15	05K146A	7	300–550	0.57	0.81	6.7	21.1±1.3	4.86	22.8±1.8	5.3±0.4
	05K147A	8	250–550	0.61	0.83	9.9	24.2±1.2	5.58		
	05K149A	7	300–550	0.62	0.79	6.2	22.8±1.5	5.25		
	05K151A	7	300–550	0.66	0.79	6.4	25.1±1.3	5.78		
	05K152A	8	250–550	0.63	0.83	17.4	21.2±0.6	4.89		

ited the recording of a reliable k-T curve.

3.3 Hysteresis and IRM measurements

Hysteresis measurements at room temperature were performed on all studied samples using the AGFM 'Micromag' apparatus in fields up to 1.55 Tesla. Saturation remanent magnetization (J_{rs}), saturation magnetization (J_s), and coercitive force (H_c) were all calculated after a correction for the paramagnetic contribution. The coercivity of remanence (H_{cr}) was determined by applying a progressively increasing backfield after saturation. Some typical hysteresis plots are shown in Fig. 2. No potbellied and wasp-waisted behaviors were detected near the origin (Tauxe *et al.*, 1996), which probably reflects a very restricted range of magnetic coercivities. The ratios of hysteresis parameters indicate that all samples fall in the pseudo-single domain (PSD) grain size region (Day *et al.*, 1977), probably indicating a mixture of multidomain (MD) and a significant amount of single domain (SD) grains (Dunlop, 2002). It is worth noting that several problems arise when using the Day diagram to discriminate the true magnetic structure (Goguitchaichvili *et al.*, 2001a): (1) natural rocks are complex magnetic systems that contain grains of variable sizes, coercivities, and even distinct magnetic phases. Thus, generalizations based on studies of synthetic materials with established chemical composition are probably open to discussion. (2) Natural rocks may contain other solid solutions, such as ilmeno-hematites (titanohematites) or titanomaghemites. In these cases, the Day plot cannot be used. (3) When superparamagnetic grains are present, they can contribute to induced magnetization by deviating artificial hysteresis parameters towards PS or MD regions on the Day diagram. Thus, we believe that the Day diagram does not fully reflect the magnetic structure discrimination in natural rocks and only yields the 'average' domain state.

The corresponding isothermal remanence (IRM) acquisition curves were found to be very similar for all samples. Saturation was reached in moderate fields of the order of 150–200 mT, which points to some spinels as remanence carriers.

4. Remanence Properties

4.1 Determination of paleodirections

The remanent magnetization was measured with both JR-5A and JR-6 spinner magnetometers (nominal sensitivity $\sim 10^{-9}$ A m^2) and the measurements recorded after remanence had been stabilized. Both alternating field (AF) demagnetization using a laboratory-constructed AF-demagnetizer and stepwise thermal demagnetization up to 550–570°C using a non-inductive Schonstedt furnace were carried out. During thermal demagnetization, the low-field susceptibility at room temperature was measured after each step using a Bartington susceptibility meter.

We retrieved a stable paleomagnetic component in most of the units studied (Fig. 3). Small secondary components were easily removed by applying 10 mT or 200–250°C, with the greater part of the remanent magnetization being removed at temperatures between 500 and 550°C (Fig. 3, sample 05K069), which indicates, once again, that low-Ti titanomagnetites are the carriers of the magnetization. The median destructive fields (MDF) range mostly from 45 to 55 mT, suggesting that 'small' PSD grains are responsible for magnetization (Dunlop and Özdemir, 1997). Evidence of secondary magnetization was detected in a few samples (sample 05K106, Fig. 3). However, the primary, characteristic magnetization could be retrieved after applying 40 mT peak alternating fields. We believe that the secondary magnetization revealed by this sample is viscous in origin (viscosity index 11.8%), but we have no elements to assign this overprint to chemical or lightning processes. We noted, however, that this overprint was removed at 250°C during conventional thermal demagnetization (not shown), which is compatible to the blocking temperatures of viscous remanence (Dunlop and Özdemir, 1997).

A characteristic magnetization direction was determined by the least squares method (Kirschvink, 1980), with five to ten points being taken in the principal component analysis for this determination. Directions were averaged by unit, and the statistical parameters were calculated assuming a Fisherian distribution (Table 1).

4.2 Paleointensity determination

Paleointensity experiments were carried out under air using a MDT80 paleointensity oven. The remanence measurements were performed in a field-free environment. Temperature reproducibility between two heatings to the same temperature was generally within 3°C up to 450°C and 2°C above. The intensity of the laboratory field was 30 μT, which was taken to be a precision of better than 0.15 μT.

We used the Coe version of the Thellier and Thellier (1959) method (Coe, 1967; Coe *et al.*, 1978) with sliding natural remanent magnetization-thermoremanent magnetization (NRM-TRM) checks (Prévot *et al.*, 1985). At each temperature step the samples were heated twice: in zero field for the first heating and in the presence of a field for the second heating. The pTRM checks were performed after every second step throughout the whole experiment. So-called *pTRM tail* checks are often incorporated during the measurements (Riisager *et al.*, 2002) to detect the presence of MD magnetic grains. We prefer avoiding this procedure because of the additional heatings that are required. Rather, we believe that the contributions of grains with a MD magnetic structure should be detected before the Thellier experiments as part of suitable sample selection for paleointensity measurements.

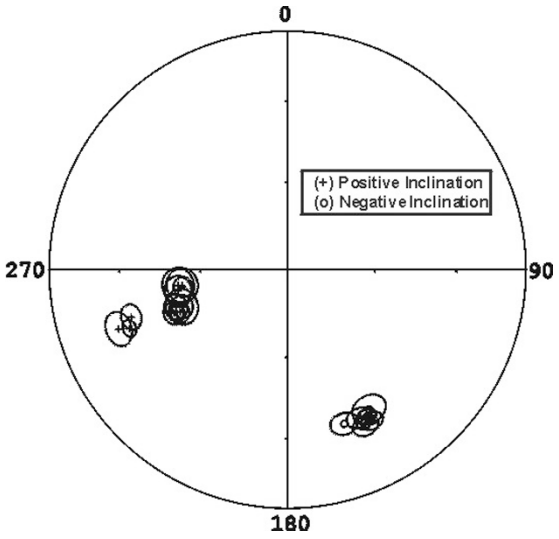

Fig. 5. Equal area projections of the flow mean characteristic paleodirections obtained in this study. Circles/crosses denote the negative/positive inclination, respectively.

Based on the paleodirectional and rock-magnetic results, 71 samples belonging to 15 lava flows that yielded stable, essentially one-component magnetizations with blocking temperatures compatible with a Ti-poor titanomagnetite phase, low viscosity indices (lower than 3%), and nearly reversible k-T curves were pre-selected for Thellier paleointensity experiments. Paleointensity data for the classical Arai-Nagata (Nagata *et al.*, 1963) plot are shown in Figs. 4(a) and (b), and the results are given in Table 2. We accepted only determinations that fulfilled the following criteria: (1) the determination was obtained from at least six NRM-TRM points corresponding to a NRM fraction larger than 1/3; (2) the quality factor (Coe *et al.*, 1978) was about 5 or more; (3) positive 'pTRM' checks, i.e., the deviation of the pTRM' checks, were less than 15%. The directions of the NRM remaining at each step obtained from the paleointensity experiments are reasonably linear and point to the origin. No deviation of remaining NRM directions towards the direction of the applied laboratory field was observed (Figs. 4(a) and (b)).

While procedures for determining the direction of the paleomagnetic field are now more or less standardized, significant inter-laboratory differences on how to best obtain reliable estimates of paleomagnetic field intensity still exist. Valet and Herrero-Bervera (2000) provided experimental evidence that the zero field demagnetization performed prior to the TRM in the Coe version prevents visualization of the possible acquisition of chemical remanent magnetiza-

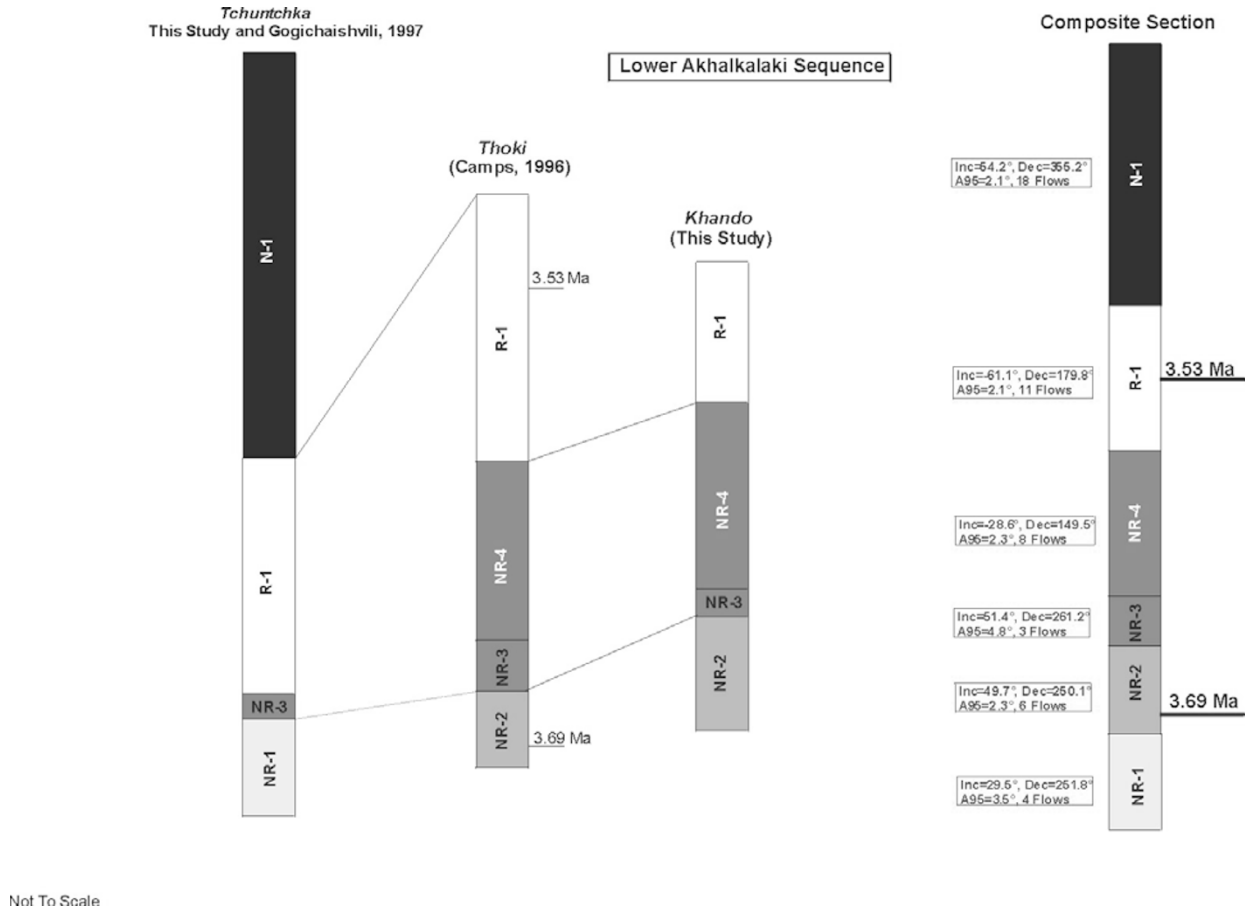

Fig. 6. A tentative magnetostratigraphic correlation between the main studied profiles.

tion (CRM). In order to monitor potential CRM production, we calculated the ratio of potential CRM(T) to the magnitude of NRM(T) for each double heating step in the direction of the laboratory field during heating at temperature T (Goguitchaichvili *et al.*, 1999b). The values of angle γ—the angle between the direction on characteristic remanent magnetization (ChRM) obtained during the demagnetization in the zero field and that of the composite magnetization (equal to NRM(T) if CRM(T) is zero) are all $<8^\circ$, which attests that no significant CRM was acquired during the laboratory heating steps.

Ultimately, only 37 samples from ten individual lava flows yielded acceptable paleointensity estimates. For these samples, the NRM fraction f used for determination ranges from 0.46 to 0.88 (Table 2), and the quality factor q ranges from 4.4 to 59.6, being generally greater than 5. For the remaining samples, the main reason for failure of Thellier paleointensity experiments was a typical 'concave-up' behavior (Levi, 1977; Dunlop and Özdemir, 1997) possibly related to the presence of MD grains. An important loss of NRM was observed without any noticeable TRM acquisition (Fig. 4(b), sample 05K075B). Alternatively, this phenomenon can be due to irreversible variations of coercive force (Kosterov *et al.*, 1998) at low temperatures and can be interpreted as transformation from a SD 'metastable' state to polydomain state, which results in a large NRM loss without any correlated TRM acquisition during the subsequent cooling.

5. Discussion and Main Results

The average flow paleodirections are very precisely determined (Table 1). The α_{95} and k values obtained point to small within-site dispersion and, consequently, to high-quality data (Fig. 5). All flows belonging to lower the Tchuntchka section yielded intermediate polarity. The paleodirections found here are rather similar to those obtained from the Thoki original section. The Khando sequence is characterized by almost the same (intermediate) paleodirections (Figs. 5 and 6) at its lower part (eight lavas). The upper lavas are characterized by unusually shallow inclinations (see also Table 1).

It is apparent that each lava flow does not record an independent measurement of the geomagnetic field. For this reason, samples from several flows that record the same field direction have been averaged together, and the resulting direction is given as a 'directional group' using original codes (NR for intermediate flows and R or N for reverse or normal polarities, respectively) of Sologashvili (1986). These directional groups were defined following the criteria of Mankinen *et al.* (1985) (see also Prévot *et al.*, 1985; Camps *et al.*, 1996). In general, if the flow-mean paleodirections of two or more flows showed no systematic trends and their ovals of 95% confidence overlapped, they were considered to record the same field directions.

The composite section we present here is a result of field observations, preliminary NRM measurements performed in early 1980s (Sologashvili, 1986) using an astatic mag-

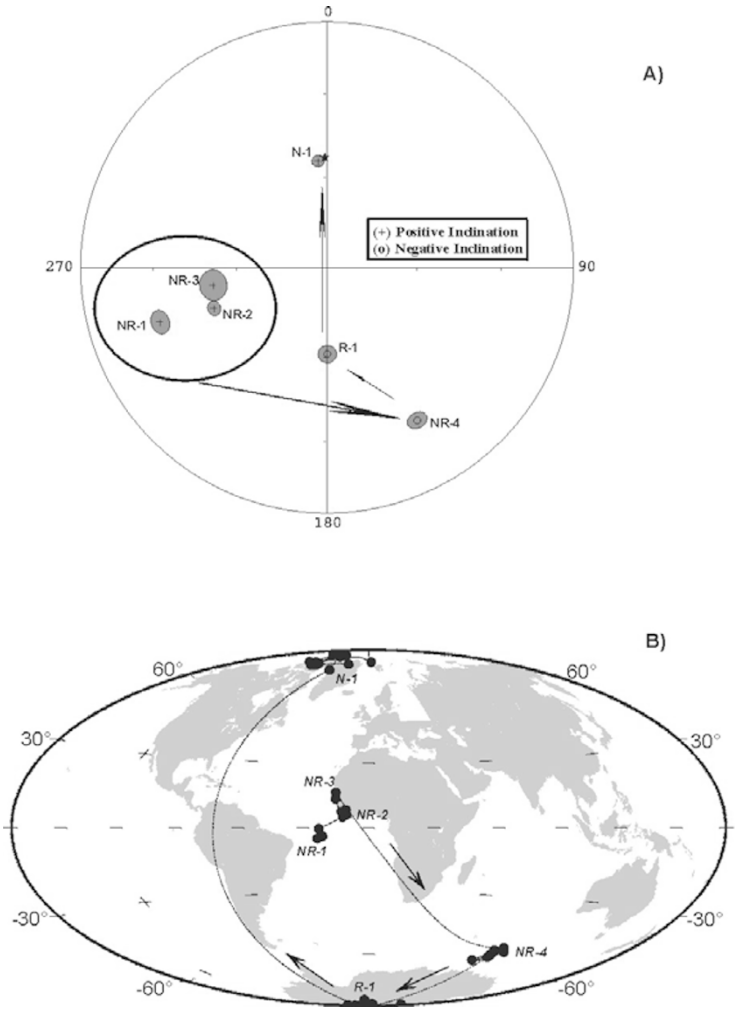

Fig. 7. (a) Equal area projections of the flow mean characteristic paleodirections of Akhalkalaki volcanics. Circles/crosses denote the negative/positive inclination, respectively. (b) The path of the virtual geomagnetic pole positions.

netoemeter, and tentative between-site magnetic correlation (Fig. 6). The paleomagnetic record starts with directional group NR1 defined by four lava flows from the Tchuntchka lower sequence (see also Figs. 7(a) and 8). The NR2 (six flows) and NR3 (three flows) directional groups yielded rather similar paleodirections, and both are represented in the Khando and Thoki sites, while NR2 is absent in Tchuntchka. The same is true for the thick NR4 zone (eight flows). In contrast, the reverse polarity zone R1 (11 lava flows) is a common feature for all three sections. We also note that NR1 lavas strongly deviate (almost 40°) from the expected Pliocene mean paleodirections (Inc $= 57.7°$ and Dec $= 6°$ after Sologashvili, 1986) and thus should be considered as distinct to R1 zone. The relatively thick normal polarity zone (N1, 18 flows) is only present in the Tchuntchka section (Fig. 6). It seems that this section was built up by distinct sources during the formation of the present volcanic edifice, which is actually a very common feature of Akhalkalaki plateau volcanism where several volcanic sources acted (and co-existed) almost simultaneously (Maissuradeze, 1989). Taking all available radiometric ages (Camps *et al.*, 1996; see also Figs. 6 and 7(a)) and new paleomagnetic data into consideration, it would seem that the Gilbert-Gauss (R-N) reversal is recorded at the upper part of the composite sequence. Lower intermediate polarity flows possibly represent a kind of precursor of this reversal, similar to the Matuyama-Brunhes geomagnetic transition (Quideleur *et al.*, 2002; Petronille *et al.*, 2005; Gratton and Shaw, 2007). The occurrence of such a geomagnetic precursor was also documented by Herrero-Bervera and Valet (2005) for older transitions. More evidence for a geomagnetic event just prior to the M-B reversal comes from sedimentary records (Kent and Schneider, 1995; Hartl and Tauxe, 1996; Carcaillet *et al.*, 2004). These authors observed shallow inclinations together with a drop in relative paleointensity about 15 ky prior to the M-B transition. Taking all of these results into account, it is possible to speculate that the precursor may be a general feature for all pre-transitional geomagnetic regimes.

The paths of virtual geomagnetic pole (VGP) positions (Fig. 7(b)) do not seem to match to any of the preferred longitude sectors (Laj *et al.*, 1991) provided by sedimentary records. There is some similarity, however, with the paleomagnetic record obtained from a reversal at about 3.6 Ma (presumably Gilbert-Gauss transition; Herrero-Bervera and Valet, 2005) revealed in the Waianae sequence (Oahu, Hawaii). The absolute paleointensity is drastically reduced during the transitional magnetic event, as observed world-

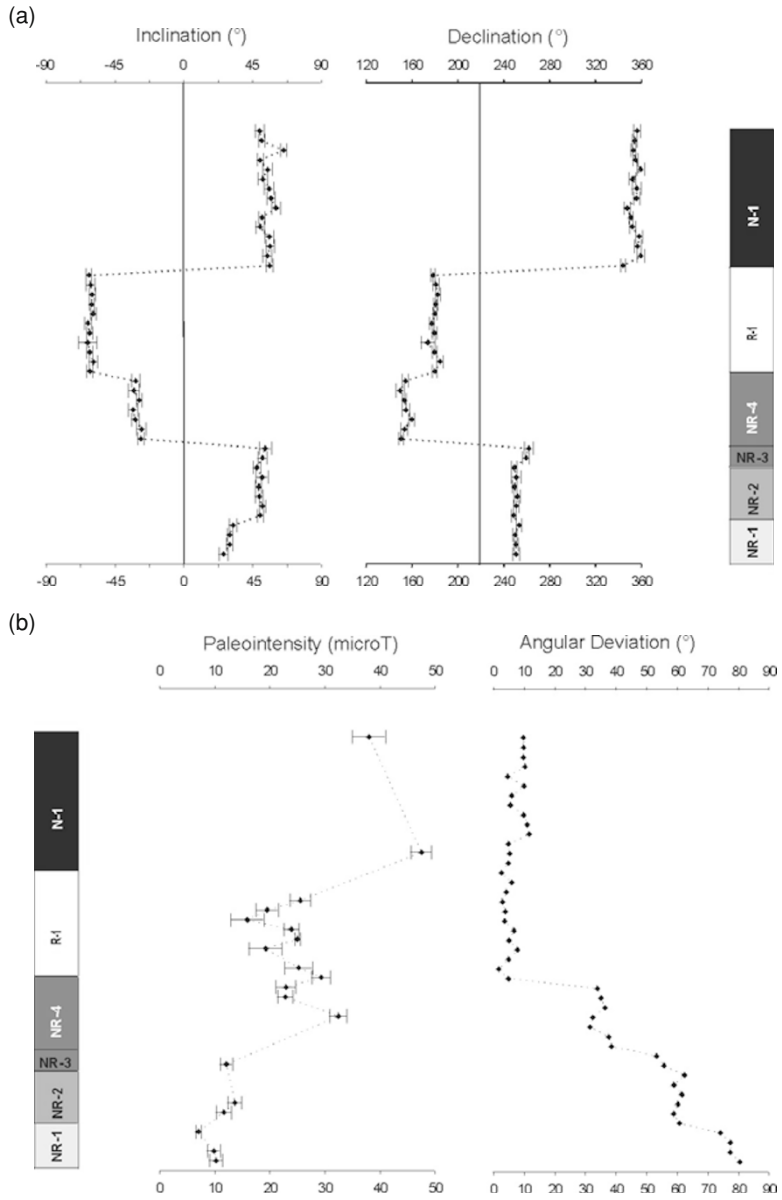

Fig. 8. Flow mean inclination, declination (a), angular deviation from expected paleodirections, and absolute paleointensity (b) for each flow of the Akhalkalaki composite section against elevation.

wide for all excursions and reversals (Fig. 8). The almost linear evolution from the transitional to normal geomagnetic regime and a relatively rapid restoration of a stable dipole intensity are interesting features of the paleointensity record obtained in this study. These features were also observed at Waianae (Herrero-Bervera *et al*., 2005), La Palma (Quideleur *et al*., 2002), Iceland (Goguitchaichvili *et al*., 1999b), and Steens Mountain (Prévot *et al*., 1985). Our paleointensity data do not confirm the presence of an unusually high post-intermediate paleointensity, as was detected in Kauai (Bogue and Paul, 1993) and Greenland (Riisager and Abrahamsen, 2000). Moreover, two detailed post-intermediate records, the Gauss-Matuyama transition studied by Tanaka *et al*. (1995) and Reunion-Matuyama studied by Goguitchaichvili *et al*. (1999c) both yielded similar (relatively low) values of the post-transitional paleofield strength. These results suggest that the regime of the geodynamo following reversals or excursions may vary significantly from one geomagnetic event to the next without any apparent systematic features, as has already been suggested by Goguitchaichvili *et al*. (2001b).

Acknowledgments. The financial support was provided by Junta de Castilla y Leon (Spain) and CONACYT project no. 54956 (Mexico).

References

Bogue, S. W. and H. A. Paul, Distinctive field behaviour following geomagnetic reversals, *Geophys. Res. Lett.*, **20**, 2399–2402, 1993.

Camps, P., G. Ruffet, V. P. Scherbakov, V. V. Scherbakova, M. Prévot, A. Moussine-Pouchkin, L. Sholpo, A. Goguitchaichvili, and B. Asanidze, Paleomagnetic and geocronological study of a geomagnetic field reversal or excursion recorded in Pliocene volcanic rocks from Georgia (lesser Caucasus), *Phys. Earth Planet. Inter.*, **96**, 41–59, 1996.

Carcaillet, J. T., D. Bourles, and N. Thouveny, Geomagnetic dipole moment and ^{10}Be production rate intercalibration from authigenic ^{10}Be/^{9}Be for the last 1.3 Ma, *Geochem. Geophys., Geosyst.*, **5**, doi 1029/2003GC000641, 2004.

Coe, R., Paleointensity of the Earth's magnetic field determined from

Tertiary and Quaternary rocks, *J. Geophys. Res.*, **83**, 1740–1756, 1967.
Coe, R. S., S. Grommé, and E. A. Mankinen, Geomagnetic paleointensities from radiocarbon-dated lava flows on Hawaii and the question of the Pacific nondipole low, *J. Geophys. Res.*, **83**, 1740–1756, 1978.
Cox, A., Lengths of geomagnetic polarity intervals, *J. Geophys. Res.*, **73**, 3247–3260, 1968.
Day, R., M. Fuller, and V. A. Schmidt, Hysteresis properties of titanomagnetites: Grain-size and compositional dependence, *Phys. Earth Planet. Inter.*, **13**, 260–267, 1977.
Dunlop, D. J., Theory and application of the Day plot (Mrs/Ms versus Hcr/Hc), Theoretical curves and tests using titanomagnetite data, *J. Geophys. Res.*, **107**, doi:10.1029/2001JB000486, 2002.
Dunlop, D. and Ö. Özdemir, *Rock-Magnetism, fundamentals and frontiers*, 573 pp., Cambridge University Press, 1997.
Goguitchaichvili, A., D. Sologachvili, M. Prévot, M. Calvo, E. S. Pavlenichvili, G. Maissuradze, and E. Schnepp, Paleomagnetic and rock-magnetic study of a Pliocene volcanic section in south Georgia (Caucasus), *Geol. Mijnbouw*, **76**, 135–143, 1997.
Goguitchaichvili, A., M. Prévot, J. M. Dautria, and M. Bacia, Thermodetrital and crystalline magnetizations in an Icelandic hyaloclastite, *J. Geophys. Res.*, **104**, 29219–29239, 1999a.
Goguitchaichvili, A., M. Prévot, N. Roberts, and J. Thompson, An attempt to determine the absolute geomagnetic field intensity in Southwestern Iceland during the Gauss-Matyama reversal, *Phys. Earth Planet. Inter.*, **115**, 53–66, 1999b.
Goguitchaichvili, A., M. Prévot, and P. Camps, No evidence for strong fields during the R3-N3 Icelandic geomagnetic reversals, *Earth Planet. Sci. Lett.*, **167**, 15–34, 1999c.
Goguitchaichvili, A., J. Morales, and J. Urrutia-Fucugauchi, On the use of thermomagnetic curves in paleomagnetism, *C. R. Acad. Sci., Earth Planet. Sci.*, **333**, 699–704, 2001a.
Goguitchaichvili, A., P. Camps, and J. Urrutia-Fucugauchi, On the features of the geodynamo following reversals or excursions, *Phys. Earth Planet. Inter.*, **124**, 81–93, 2001b.
Gratton, M. and J. Shaw, Absolute palaeointensity variation during a precursor to the Matuyama-Brunhes transition recorded in Chilean lavas, *Earth Planet. Sci. Lett.*, **162**(1–2), 61–72, 2007.
Gubbins, D., The distinction between geomagnetic excursions and reversals, *Geophys. J. Int.*, **137**, F1–F3, 1999.
Hartl, P. and L. Tauxe, A precursor to the Matuyama/Brunhes transition—field instability as recorded in pelagic sediments, *Earth Planet. Sci. Lett.*, **138**, 121–135, 1996.
Herrero-Bervera, E. and J. P. Valet, Absolute paleointensity and reversal records from the Wainanae sequence (Oahu, Hawaii, USA), *Earth Planet. Sci. Lett.*, doi:10.1016/j.epsl.2005, 2005.
Kent, D. V. and D. A. Schneider, Correlation of paleointensity variation records in the Brunhes/Matuyama polarity transition interval, *Earth Planet. Sci. Lett.*, **129**, 135–142, 1995.
Kirschvink, J. L., The least-square line and plane and analysis of palaeomagnetic data, *Geophys. J. R. Astron. Soc.*, **62**, 699–718, 1980.
Knudsen, M. F., N. Abrahamsen, and P. Riisager, Paleomagnetic evidence from Cape Verde Islands basalts for fully reversed excursions in the Brunhes Chron, *Earth Planet. Sci. Lett.*, **206**, 199–214, 2003.
Kosterov, A., M. Perrin, J. M. Glen, and R. S. Coe, Paleointensity of the Earth's magnetic field in early Cretaceous time: The Paraná Basalt, Brazil, *J. Geophys. Res.*, **103**, 9739–9753, 1998.
Laj, C., A. Mazaud, R. Weeks, and E. Herrero-Bervera, Geomagnetic reversal paths, *Nature*, **351**, 347–350, 1991.
Levi, S., The effect of magnetite particle size in paleointensity determination of the geomagnetic field, *Phys. Earth Planet. Inter.*, **13**, 245–258, 1977.
Maissuradze, G., Antropogene of Anti-Caucasus, *Paleogr. Paleoclim. Paleoecol.*, **72**, 53–61, 1989.
Mankinen, E. A., M. Prévot, C. S. Grommé, and R. Coe, The Steens Mountain (Oregon) geomagnetic polarity transition 1, Directional history, duration of episodes and rock-magnetism, *J. Geophys. Res.*, **90**, 10393–10416, 1985.
Merrill, R. T. and P. L. McFadden, Geomagnetic field stabuility: Reversal events and excursions, *Earth Planet. Sci. Lett.*, **121**, 57–69, 1994.
Milanovski, E. E., *Neotectonics of the Caucasus*, 278 pp., Nedra, 1978 (in Russian).
Mochizuki, N., H. Tsunakawa, H. Shibuya, J. Cassidy, and I. E. M. Smith, Palaeointensities of the Auckland geomagnetic excursions by the LTD-DHT Shaw method, *Phys. Earth Planet. Inter.*, **154**, 168–179, 2006.
Mochizuki, N., H. Tsunakawa, H. Shibuya, T. Tagami, A. Ozawa and I. E. M. Smith, Further K-Ar dating and paleomagnetic study of the Auckland geomagnetic excursions, *Earth Planets Space*, **59**, 755–761, 2007.
Nagata, T., R. M. Fisher, and K. Momose, Secular variation of the geomagnetic total force during the last 5000 years, *J. Geophys. Res.*, **68**, 5277–5281, 1963.
Özdemir, Ö., Inversion of titanomaghemites, *Phys. Earth Planet. Inter.*, **65**, 125–136, 1987.
Petronille, M., A. Goguitchaichvili, B. Henry, L. Alva-Valdivia, J. Rosas-Elguera, M. Rodríguez Ceja, and M. Calvo-Rathert, Paleomagnetism of Ar-Ar dated lava flows from the Ceboruco-San Pedro volcanic field (western Mexico): Evidence for the Matuyama-Brunhes transition precursor and a fully reversed geomagnetic event in the Brunhes chron, *J. Geophys. Res.*, **110**, B08101, doi:10.1029/2004jb003321, 2005.
Prévot, M., R. S. Mainkinen, S. Grommé, and A. Lecaille, High paleointensity of the geomagnetic field from thermomagnetic studies on rift valley pillow basalts from the middle Atlantic ridge, *J. Geophys. Res.*, **88**, 2316–2326, 1983.
Prévot, M., R. S. Mainkinen, R. S. Coe, and S. Grommé, The Steens Mountain (Oregon) geomagnetic polarity transition 2. Field intensity variations and discussion of reversal models, *J. Geophys. Res.*, **90**, 10417–10448, 1985.
Quidelleur, X., J. Carlut, P. Y. Gillot, and V. Soler, Evolution of the geomagnetic field prior to the Matuyama-Brunhes transition: radiometric dating of a 820 ka excursion at La Palma, *Geophys. J. Int.*, **151**, F6–F10, 2002.
Riisager, P. and N. Abrahamsen, Palaeointensity of West Greenland Palaeocene basalts: asymmetric intensity around the C27n-C26r transition, *Phys. Earth Planet. Inter.*, **118**, 53–64, 2000.
Riisager, P., J. Riisager, N. Abrahamsen, and R. Waagstein, Thellier paleointensity experiments on Faroes Flood Basalts: Technical aspects and Geomagnetic Implications, *Phys. Earth Planet. Inter.*, **131**, 91–100, 2002.
Singer, B. S., M. K. Relle, K. A. Hoffman, A. Battle, C. Laj, H. Guillou, and J. Carracedo, Ar/Ar ages from transitionally magnetized lavas on La Palma, Canary Island, and the geomagnetic instability timescale, *J. Geophys. Res.*, **107**(B11), 10.1029/2001JB001613, 2002.
Sologashvili, J., Paleomagnetism of Neogene volcanic units of Georgia, Phd Thesis, Tbilisi State University, 168 pp., 1986.
Tanaka, H., M. Kono, and S. Kaneko, Paleosecular variation of direction and intensity from two Pliocene-Pleistocene lava sections in Southwestern Iceland, *J. Geomag. Geoelectr.*, **47**, 89–102, 1995.
Tauxe, L., Sedimentary records of relative paleointensity: Theory and practice, *Rev. Geophys.*, **31**, 319–354, 1993.
Tauxe, L., T. A. T. Mullender, and T. Pick, Pot-bellies, wasp-waists and superparamagnetism in magnetic hysteresis, *J. Geophys. Res.*, **95**, 12337–12350, 1996.
Thellier, E. and O. Thellier, Recherches géomagnetiques sur les coulees volcaniques d'Auvergne, *Ann. Geophys.*, **1**, 37–52, 1944.
Thellier, E. and O. Thellier, Sur l'intensité du champ magnétique terrestre dans le passé historique et géologique, *Ann. Géophys.*, **15**, 285–376, 1959.
Valet, J. P. and E. Herrero-Bervera, Paleointensity experiments using alternating field demagnetization, *Earth Planet. Sci. Lett.*, **177**, 43–58, 2000.
Valet, J. P. and E. Herrero-Bervera, Some characteristics of geomagnetic reversals inferred from detailed volcanic records, *C. R. Geosci.*, **335**, 79–90, 2003.

A. Goguitchaichvili (e-mail: avto@geofisica.unam.mx), M. A. Cervantes, M. Calvo Rathert, P. Camps, J. Sologashvili, and G. Maissuradze